

# Assessing Salinization of Coastal Groundwater by Tidal Action: The Tropical Wouri Estuary, Douala, Cameroon

Goabaone J. Ramatlapeng<sup>1</sup>, Eliot A. Atekwana<sup>1\*</sup>, Hendratta N. Ali<sup>2</sup>, Isaac K. Njilah<sup>3</sup> and Gustave R. N. Ndondo<sup>4</sup>

<sup>1</sup>Department of Earth Sciences, University of Delaware, Newark, DE 19716

<sup>2</sup>Department of Geosciences, Fort Hays State University, Hays, KS 67601

<sup>3</sup>Department of Earth Sciences, University of Yaoundé I, Yaoundé, Cameroon

<sup>4</sup>Department of Geosciences, University of Douala, Douala, Cameroon

\*Corresponding author (University of Delaware, Delaware, USA): Tel.: +1 302.831.8106; Fax: +1 302.831.4158; Email address: eatekwan@udel.edu

## Highlights

- We assessed tide-induced salinization of coastal groundwater by the Wouri Estuary
- Groundwater 250 m from the shore is not affected by tide-induced salinization
- Groundwater in the coastal Douala aquifer have similar ionic ratios and origin
- Groundwater salinization is geogenic, likely from connate water in the aquifer units

## ABSTRACT

*Study region:* Douala, Cameroon, West Africa

20 *Study focus:* Salinity of shallow coastal groundwater in Douala, Cameroon impairs its use for  
21 drinking and industrial purposes. Previous studies suggest that salinization is from tidal flooding  
22 from the Wouri Estuary. We aimed to test the tidal origin of groundwater salinization by  
23 conducting a time series investigation of water level and salinity, and assessed the stable water

24 isotopes ( $\delta^{18}\text{O}$  and  $\delta\text{D}$ ) and major cations ( $\text{Ca}^{2+}$  and  $\text{Mg}^{2+}$ ) in groundwater and adjacent  
25 estuarine tidal creek. During the time series measurements, we pumped groundwater for over 5  
26 tidal cycles to induce flow into a test well.

27 *New hydrologic insights for the region:* The time-series groundwater level mimicked water level  
28 changes in the estuary. However, the temporal salinity in groundwater did not correspond to tidal  
29 salinity changes of estuarine water, indicating that estuarine water did not intrude groundwater.  
30 The  $\delta^{18}\text{O}$  and  $\delta\text{D}$  of the groundwater and estuarine samples are collinear and fall along the local  
31 meteoric water line of Douala and had d-excesses of  $>10$ , indicating a non-evaporated rain  
32 recharge of groundwater or lack of salinization by evapoconcentration. The salinity- $\delta^{18}\text{O}$   
33 relationship showed that the origin of salinity in the coastal groundwater aquifer is not from  
34 seawater intrusion. The  $\text{Mg}^{2+}/\text{Ca}^{2+}$  ratios of  $<1$  in groundwater compared to 6-8 in estuarine  
35 water support the non-seawater origin of groundwater salinity. We conclude that the salinity of  
36 coastal groundwater in Douala is not affected by tide-induced salinization from the adjacent  
37 Wouri Estuary but by geogenic sources in the aquifer.

38

39 *Keywords:* Coastal groundwater; groundwater salinization; time series analysis; Wouri Estuary;  
40 Cameroon

41

## 42 1. Introduction

43 The quality of coastal groundwater is a crucial factor in water resource management and  
44 sustainability (Lee and Song et al., 2007; Werner et al., 2013; Mirzavand et al., 2018; Mirzavand  
45 et al., 2020; Ouhamdouch et al., 2021). Salinization is an important process that causes quality  
46 deterioration in groundwater in coastal regions. Studies conducted in coastal settings show that

47 groundwater salinization occurs from seawater intrusion induced by groundwater overdraft  
48 (Melloul and Goldenberg, 1997; Demirel, 2004; Pulido-Laboeuf, 2004; Jørgensen et al., 2008;  
49 Werner et al., 2013; Ouhamdouch et al., 2017; Kanagaraj et al., 2018), tidal flooding and storm  
50 surges (Mao et al., 2001), geochemical processes such as water-rock interaction, cation  
51 exchange, carbonate and mineral dissolution, evaporation of freshwater and mixing with saline  
52 connate water in the sedimentary formations (Hem, 1985; Aquilina et al., 2002; Amiri et al.,  
53 2016; Mirzavand et al., 2020) and from anthropogenic pollution (Cary et al., 2015; Bahir and  
54 Ouhamdouch, 2020).

55 The effective management of coastal groundwater resources depends on the understanding of  
56 sources of salinity in the groundwater. However, the multiplicity of mechanisms of salinization  
57 confound the determination of the origin of salinity in coastal groundwater (Mirzavand et al.,  
58 2020). Hence, many studies have utilized different methods to identify saline coastal  
59 groundwater and determined their salinization mechanisms. Geophysical methods (e.g., electrical  
60 resistivity) have been used to detect salinity differences between saline and fresh groundwater  
61 and their interface (Mirzavand, 2018, 2020). Although the commonly used electrical resistivity  
62 method show salinity disparities between saline and fresh groundwater, the method cannot  
63 determine the origin and mechanism of groundwater salinization (Mirzavand 2020). Thus, to  
64 determine the source(s) of salinity and mechanisms of groundwater salinization, studies have  
65 used hydrogeochemical modeling techniques such as PHREEQE and faces evolution diagrams  
66 (Giménez-forcada, 2010) and geochemical tracers such as salinity, minor and major ions (Alcalá  
67 and Custodio, 2008; Harkness et al., 2017; Isawi et al., 2016; Mirzavand, 2018; Amiri et al.,  
68 2016; 2021). Hydrogeochemical modelling allow researchers to simulate mixing and reaction  
69 pathways (PHREEQE), classify water (Piper diagrams) and decipher intrusion and freshening

70 phases (hydrochemical facies evolution diagram: HFE-D). Geochemical tracers such as major  
71 ion ratios ( $\text{Na}^+/\text{Cl}^-$ ,  $\text{Br}^-/\text{Cl}^-$ ,  $\text{SO}_4^{2-}/\text{Cl}^-$ ,  $\text{Ca}^{2+}/\text{Cl}^-$ ,  $\text{B}/\text{Cl}^-$ ,  $\text{Mg}^{2+}/\text{Cl}^-$ ) have been used in studies to  
72 identify the major sources of salinity in groundwater (Alcalá and Custodio, 2008; Amiri et al.,  
73 2016; 2021). However, these ionic ratios can be affected by processes such as water-rock  
74 interaction and anthropogenic contamination which may cause problems with source  
75 identification in coastal aquifers in urbanized settings. Due to the limitations of the different  
76 approaches to identify the origin of salinity in coastal groundwater, researchers combine multiple  
77 approaches to elucidate the origin of salinity in groundwater.

78 Although groundwater salinization in coastal areas have been widely researched using  
79 different methods, few of these studies have focused on assessing the effects of salinization of  
80 groundwater by estuarine water (Mao et al., 2001; Mao et al., 2006; Lenkopane et al., 2009;  
81 Tularam and Singh, 2009; Dieng et al., 2017; Shalem et al., 2019) as a result of tidal forcing.  
82 Studies on tide-induced groundwater salinization in estuarine settings requires a unique  
83 experimental approach assessing near real time behavior of water and salinity in both  
84 groundwater and the estuary. A significant challenge to study tide-induced salinization of coastal  
85 groundwater in estuarine environments is to acquire hydrochemical data at a frequency adequate  
86 to elucidate the effects of tides in this process. Thus, there is a need to acquire data on water  
87 level (tides) and tracers of salinity (e.g., salinity, major cations) and tracers of water origin  
88 (stable oxygen ( $\delta^{18}\text{O}$ ) and hydrogen ( $\delta\text{D}$ ) isotopes) at a frequency adequate to characterize tidal  
89 effects. When tracers of salinity and water origin are collected over multiples tidal cycles, the  
90 data allows for direct comparison between the near real time behavior of the tracers in estuarine  
91 water to those in groundwater (Jones et al., 1999; Mao et al., 2006; Lenkopane et al., 2009;  
92 Currell et al., 2015; Shalem et al., 2019).

93 In this study, we investigated groundwater salinization from the coastal aquifer adjacent to  
94 the tropical Wouri Estuary (Douala, Cameroon). Groundwater in the coastal Douala aquifer  
95 serves as both a supplementary and a primary source of water supply for domestic and industrial  
96 activities (Takem et al., 2010; Takem et al., 2015; Fantong et al., 2016; Ketchemen-Tandia et al.,  
97 2017; Wirmvem et al., 2017a). A study of the hydrogeochemical characteristics of surface flows  
98 and groundwater in Douala by Fantong et al. (2016) confirmed quality impacts from salinization.  
99 The groundwater salinization characterized by high chloride concentrations is attributed to tide-  
100 induced flooding by estuarine water (Mafany, 1999; Fantong et al., 2016). Tide-induced  
101 salinization adequately explains seawater contamination of coastal groundwater immediately  
102 adjacent to the coast, where high tides cause (1) higher heads relative to groundwater causing  
103 estuarine water to flow into and salinize groundwater or (2) estuarine water to overtop and flood  
104 the land surface, which subsequently infiltrates, recharges and salinize groundwater (Mao et al.,  
105 2006; Tularam and Singh, 2009; Shalem et al., 2019).

106 To test if tide-induced estuarine water head and/or flooding are responsible for estuarine  
107 water contamination of the coastal aquifer in Douala (Mafany, 1999; Fantong et al., 2016), we  
108 investigate tide induced salinization of groundwater in the Youpwe neighborhood, adjacent to  
109 the Wouri Estuary. The Youpwe neighborhood in the coastal city of Douala Cameroon (Fig. 1) is  
110 an ideal location to study estuarine salinization of groundwater. A tidal creek (Dr. Creek) forms a  
111 linear boundary between groundwater below the Youpwe neighborhood and the estuary, and can  
112 be envisioned as a linear source of estuarine water which could potentially impact shallow  
113 groundwater. We employed a combination of time series water level and salinity measurements  
114 and assessed the  $\delta^{18}\text{O}$  and  $\delta\text{D}$  and major cation ratios to track estuarine salinization of  
115 groundwater. Our objective was to ascertain if saline water from the Wouri Estuary is the cause

116 of salinization of groundwater. Our findings are important for understanding coastal groundwater  
117 salinization and contamination and for management of coastal groundwater resources in this  
118 tropical estuarine environment.

119

120 **2. Study site**

121 2.1 Location of water sampling sites

122 The groundwater and estuarine water (Dr. Creek) investigated in this study are located in the  
123 Youpwe neighborhood near the head of the Wouri Estuary in the city of Douala, Cameroon (Fig.  
124 1). The Wouri Estuary ( $3^{\circ}49'$  -  $4^{\circ}04'$  N and  $9^{\circ}20'$  -  $9^{\circ}40'$  E) is located in the Gulf of Guinea on  
125 the Atlantic coast of Cameroon's coastline plain (Fig. 1a). The Wouri Estuary comprises open  
126 water of approximately  $1200 \text{ km}^2$  and extensive ( $1750 \text{ km}^2$ ) mangrove forests (Simon and  
127 Raffaelli, 2012; Ndongo et al., 2015; Fossi Fotsi et al., 2019). Freshwater discharge into the  
128 Wouri Estuary are from the Wouri River at the head and the Dibamba River and Mungo River  
129 about 15 km from the head (Fig. 1a).

130

131 2.2. Climate

132 Douala has a humid equatorial climate characterized by a rainy season that spans from April  
133 to October and a dry season that spans from November to March (e.g., Fantong et al., 2016). The  
134 mean annual precipitation is 4000 mm and rainfall amounts peak in June and September. During  
135 the rainy season, saturated air masses blow from the Gulf of Guinea. During the dry season, the  
136 Harmattan winds blow southwestward from the Sahara Desert causing low humidity and high  
137 temperature conditions. The daily temperature ranges between 23 and 33 °C.

138

139 2.3. Geological setting

140 The study area is in the Phanerozoic Cretaceous-Quaternary Douala Basin (Dumort, 1968;  
141 Regnoult, 1986). The Douala Basin consists of up to 5 km thick sedimentary sequence of  
142 unconsolidated and semi-consolidated rocks which overlie a Precambrian basement (Regnoult,  
143 1986; Tamfu et al., 1995). The vertical succession consists of the Moundeck, Logbaba, Nkappa,  
144 Souelaba, Matanda and Wouri Formations (Regnoult, 1986). The lithologic composition of the  
145 Moundeck Formation varies from shale at the top, through medium sized sand, to basal  
146 conglomerate that overlie the Precambrian crystalline basement. The Logbaba Formation is shale  
147 that intercalates with fossiliferous limestone and gravelly sand. The Nkappa Formation is  
148 primarily shale-rich in channel-filled sands. The Souelaba Formation is composed of marls,  
149 sandy shale, calcareous sandstone and ferruginous limestone. The mineral phases in the Nkappa  
150 and Souelaba Formations include smectite, halloysite, chlorite, feranhydrite, calcite, ilmenite,  
151 muscovite, K-feldspar, gypsum, pyrite, and corundum (Ngon et al., 2016). The Matanda  
152 Formation comprises of shale, overlain by coarse-grained sand that intercalate with Tertiary  
153 basalts from Mount Cameroon lava flows. The Wouri Formation is comprised of coarse-grained  
154 sand and gravel, intercalated with ferruginous clay dominated by quartz and varying proportions  
155 of ilmenite, magnetite, muscovite, sillimanite, epidote and sphene (Regnoult, 1986).

156

157 2.4. Groundwater hydrogeology

158 The sedimentary sequence in the Douala Basin hosts a deep and a shallow aquifer. The deep  
159 aquifer consists of the Basal Sandstones of the Cretaceous Moundeck Formation, the Logbaba  
160 Formation and the Paleocene Sands of the Nkappa Formation. The Basal Sandstones aquifer unit  
161 is confined by the underlying Precambrian granites and the upper Paleocene Sands unit is

162 confined by the impermeable marine shales of the Souelaba Formation (Regnoult, 1986; Mafany,  
163 1999). The Paleocene sand aquifer is 200 m thick and is exploited by bore holes (Djeuda-  
164 Tchapnga et al., 2001). The shallow aquifer unit is unconfined and composed of Pleistocene  
165 sands and alluvium belonging to the Matanda Formation and the Wouri Formation (Regnoult,  
166 1986). The thickness of the aquifer ranges between 50 and 60 m (Djeuda-Tchapnga et al., 2001).

167 The static water level in the shallow aquifer varies from 2 to 22 m below ground surface  
168 (bgs) and drops a 4 to 16 m range in some areas due to overexploitation (Fantong et al., 2016).  
169 The storage coefficient of the shallow aquifer varies from  $2.4 \times 10^{-5}$  to  $7.4 \times 10^{-5} \text{ m}^{-1}$ ,  
170 transmissivity ranges from  $1.1 \times 10^{-2}$  to  $2 \times 10^{-3} \text{ m/s}$ , the hydraulic conductivity is from  $1.1 \times 10^{-4}$   
171 to  $1 \times 10^{-3} \text{ m/s}$  and the specific yield varies from 2.2 to 4.9 (Fantong et al., 2016). Groundwater  
172 flow in the shallow aquifer is multidirectional; from southeast to northwest, northwest to west  
173 and from northeast to south-west (Mafany, 1999). In the Youpwe neighborhood, groundwater  
174 levels are  $<1.5 \text{ m}$  bgs and groundwater flow is generally to the south, discharging into the  
175 estuary.

176

## 177 2.5. Dr. Creek hydrology

178 Dr. Creek is a tidal creek located in the head of the Wouri Estuary and is below the southern  
179 boundary of the eastern part of the city of Douala (Fig. 1a). Dr. Creek opens to the eastern side of  
180 the Wouri Estuary, and the nearly 10 km long channel is nearly perpendicular to the estuary. Dr.  
181 Creek is flanked to the north by the Youpwe neighborhood built on previously destroyed  
182 marshland and to the south by mangrove forests of the estuary (Fig. 1b). The hydrologic regime  
183 of the Dr. Creek and the Wouri Estuary is characterized by semidiurnal mixed tides, with an  
184 average range of about 3 m (Olivry, 1974; Onguene et al., 2014).

185

186 **3. Methodology**

187 3.1. Locations for groundwater and estuarine water investigation

188 We selected three locations to investigate groundwater properties (Fig. 1b and 1c). Well 1  
189 (4°0'27.16"N, 9°42'3.62"E) is a 2.5 cm diameter borehole that is 30 m deep and located 122 m  
190 from Dr. Creek. Well 1 was drilled to support commercial activities of a hotel and is not in use  
191 because of contamination by salinity. Well 2 (4°0'29.89"N, 9°42'3.20"E) is a hand dug well 3 m  
192 deep with a diameter of 1 m and is located 200 m from Dr. Creek. Well 3 (4°0'30.18"N,  
193 9°42'2.64"E) is a hand dug well 2 m deep and 0.5 m in diameter and is located 250 m from Dr.  
194 Creek. Well 2 and Well 3 are domestic wells in active use. The time series measurements in Dr.  
195 Creek were conducted near an island (4° 0'4.28"N; 9°42'3.45"E). Estuarine water was sampled  
196 for chemical and isotopic measurements from Dr. Creek were collected at 10 stations in the creek  
197 (from 3°58'37.3"- 4°00'26.6" N to 9°41'40.1"- 9°44'09.7" E) adjacent to the Youpwe  
198 neighborhood (Fig. 1b).

199

200 3.2. Time series monitoring of air temperature, barometric pressure, water level, water  
201 temperature and electrical conductivity

202 We recorded air temperature (°C) and barometric pressure with a Solinst™ barologger. The  
203 Solinst™ barologger was set to record and convert the barometric pressure in the same units as  
204 water level (m) by using a conversion factor of 0.101972 m/kPa. The barologger pressure sensor  
205 has an accuracy of +0.05 kPa and the air temperature sensor has an accuracy of + 0.05 °C and a  
206 resolution of 0.003 °C. The barologger was deployed outside the Aquarius Marina 2000 Hotel  
207 (4° 0'26.60"N, 9°42'3.35"E) and set to an altitude of 0 m above sea level (asl).

208 We used Solinst™ LTC (level, temperature, conductivity) loggers to record water level,  
209 temperature and electrical conductivity (EC) in groundwater and estuarine water. The Solinst™  
210 LTC logger records water level with an accuracy of  $\pm 0.1\%$  percentage of full scale, and is  
211 automatically temperature compensated between 0 to 40 °C. The temperature sensor of the  
212 Solinst™ LTC has an accuracy of  $\pm 0.1$  °C and a resolution of 0.1 °C. The Solinst™ LTC  
213 measures the EC using a 4-electrode conductivity sensor that operates between -20 to 80 °C, has  
214 the ability to measure on a full range of 0 to 80,000  $\mu\text{S}/\text{cm}$  with a resolution of 1  $\mu\text{S}/\text{cm}$ , and the  
215 EC is normalized to 25 °C. The EC values were converted to salinity by multiplying the EC by  
216 0.0006, which was empirically determined from a least squares regression of EC vs. salinity  
217 measured in the Douala estuary by us (Bennett, 1976). A Solinst™ LTC logger was deployed in  
218 Well 1 from 6/11/2019 at 15 h to 6/14/2019 at 10 h. The level, temperature and conductivity of  
219 groundwater in Well 1 was monitored for 19.5 h before it was subsequently pumped at 4.7  
220  $\text{m}^3/\text{minute}$  for the duration (47.5 h) of the study using a high capacity well pump. Another  
221 Solinst™ LTC logger was deployed in Dr. Creek near a small (200 m diameter) island (4°  
222 0'4.28"N; 9°42'3.45"E) in the middle of the tidal channel (Fig. 1b). The logger was deployed  
223 from 6/12/2019 at 10 h to 6/14/2019 at 10 h at 5 cm from the channel bottom in a 5.2-cm  
224 diameter perforated PVC tube.

225 The Solinst™ barologger and LTC loggers were programmed to collect data in a linear  
226 sampling mode at minute intervals. The water levels recorded by the LTC levelloggers were  
227 corrected for barometric pressure effects using the time equivalent barometric pressure values  
228 recorded by the barologger. Barometric pressure compensation is necessary because of elevation  
229 differences above and below sea level and pressure changes from storms which can introduce  
230 errors to LTC levelloggers recorded water levels.

231

232 3.3. Water sampling

233 Groundwater samples from shallow and hand dug wells (Wells 1, 2 and 3) and surface water  
234 samples from the estuary were collected using standard sampling procedures (APHA, 1985). Six  
235 samples were collected from Well 1 during well pumping at 2 h intervals on 6/13/2019 (8, 10,  
236 12, 14, 16 and 18 h). Groundwater from Well 2 and Well 3 were collected at 25 cm below the  
237 surface on 6/21/2019 by the grab technique using clean plastic buckets. Estuarine samples from  
238 Dr. Creek were collected from 15 h to 16.7 h on 7/4/2019 at 25 cm below the surface by the grab  
239 technique along a 5 km axial transect (Fig. 1b) at high tide.

240

241 3.4. Water sample analyses

242 During the water sampling, the salinity and electrical conductivity (EC) were measured in  
243 situ in groundwater and in Dr. Creek using a Hanna (HI98194) multi-parameter (pH/Oxidation-  
244 reduction potential (ORP), electrical conductivity (EC), total dissolved solids (TDS), salinity,  
245 dissolved oxygen (DO), temperature) probe. For groundwater, the outlet of the pump was  
246 directed into a large 20 L plastic bucket where the Hanna multi-parameter probe was immersed  
247 and readings were recorded after stabilization of pH, temperature and EC. For water in Dr.  
248 Creek, the Hanna multi-parameter probe was lowered to 25 cm below the surface and readings  
249 were taken after stabilization of pH, temperature and EC.

250 Groundwater was collected directly from the outlet of the hose attached to the pump. Surface  
251 water from Dr. Creek was collected at 25 cm below the surface by the grab technique. All water  
252 samples were filtered through 0.45  $\mu\text{m}$  nylon filters during collection. The sampling bottles used  
253 were rinsed with the filtered sample to be collected and then filled and capped. Water for cations

254 analysis were collected in 60 mL polypropylene bottles and acidified to a pH <2 with trace metal  
255 grade nitric acid. Water samples for isotopic analysis were collected unacidified in 25 mL glass  
256 scintillation vials with inverted cone closures. All the water samples were kept cool and  
257 transported to the University of Delaware (USA) where they were refrigerated until analyses.

258 In the laboratory, the water samples were analyzed for calcium and magnesium by  
259 Inductively Coupled Plasma Mass Spectrometer (Agilent Tech. ICP-MS:7500<sub>cx</sub> series). The  
260  $\delta^{18}\text{O}$  and  $\delta\text{D}$  were measured using a Los Gatos Research Liquid Water Isotope Analyzer (LGR  
261 LWIA). The isotopic ratios are reported in delta notation ( $\delta$ ) in per mil (‰):

262 
$$\delta (\text{\textperthousand}) = ((R_{\text{sample}} - R_{\text{standard}}) / R_{\text{standard}}) \times 1000$$

263 where R is the ratio of D/H, or  $^{18}\text{O}/^{16}\text{O}$  in the sample and standard (e.g., Brand, 2011). The  
264 standard is the Vienna Standard Mean Ocean Water (VSMOW) international standard. The  
265 precision ( $1\sigma$  standard deviation) of the LGR LWIA is better than  $\pm 0.3\text{ ‰}$  for  $\delta\text{D}$  and  $\pm 0.07\text{ ‰}$   
266 for  $\delta^{18}\text{O}$ .

267

## 268 **4. Results**

269 4.1. Time series water level, salinity and temperature in groundwater and in Dr. Creek

### 270 *4.1.1. Water level*

271 The groundwater level measured in Well 1 fluctuated by 1.1 m (Table S1). The temporal  
272 groundwater table response was sinusoidal, with peak water level or low water level separated by  
273 ~13 h (Fig. 2a). The sinusoidal behavior and the range in change of groundwater level observed  
274 for 19.5 h before pumping was the same as during pumping over 47.5 h, except for the lowering  
275 of the water table by ~1.5 m from the pumping action. Water level in Dr. Creek varied by 1.2 m

276 (Table S1). The water level reflects semidiurnal mixed tides with a periodicity of ~13 h. (Fig.  
277 2b).

278

279 *4.1.2. Salinity*

280 The salinity of groundwater in Well 1 varied between 0.62 and 0.48 psu (Table S1). The  
281 temporal salinity in Well 1 for the 19.5 h before pumping decreased only slightly from 0.62 to  
282 0.49 psu, and during pumping, the salinity was nearly constant at 0.48 psu for the 47.5 h (Fig.  
283 2c). The salinity in Dr. Creek varied by 1.4 (Table S1). The temporal changes in the salinity  
284 coincide with tidal cycles, with high salinity observed during low tides and lower salinity  
285 observed during high tides (Fig. 2d). Additionally, the salinity peaks and troughs continuously  
286 decrease slowly over time. The salinity peaks are relatively broad compared to the troughs,  
287 which are narrower and show small salinity peaks at peak high tides.

288

289 *4.1.3. Water temperature and air temperature*

290 The temperature of groundwater in Well 1 varied between 28.2 and 28.6 °C (Table S1). The  
291 temporal temperature in Well 1 for 19.5 h before pumping decreased slightly from 28.6 to 28.4  
292 °C, and during the 47.5 h of pumping, the temperature was nearly constant at 28.2 °C (Fig. 2e).  
293 The temperature in Dr. Creek ranged from 27.6 to 29.0 °C (Table S1). The temporal temperature  
294 showed small fluctuations and a general decrease (Fig. 2f). In addition, during the temporal  
295 temperature decreases, the low temperature perturbations show correspondence to the peak tides.

296 The air temperature in Youpwe varied between 24.3 and 32.8 °C (Table S1). The temperature  
297 varied on a diurnal basis with higher temperatures during the day and lower temperatures at  
298 night. The daily highs show a peak at ~10:00 h, a low at ~12:00 h and another high at 15:00 h

299 (Fig. 2g and h). From the afternoon at 15:00 h, the temperature decreases continuously to their  
300 lowest values at ~7:00 h in the morning.

301

302 4.2. Stable isotopes, salinity, and major cations in groundwater and in Dr. Creek

303 *4.2.1. Stable isotopic composition*

304 The  $\delta D$  of groundwater in Well 1 for all samples was -10 ‰ and the  $\delta^{18} O$  ranged between -  
305 2.9 and -2.7 ‰, with a mean of  $-2.8 \pm 0.1$  ‰ (Table 1). In groundwater from Well 2,  $\delta D$  and  
306  $\delta^{18} O$  composition were -10 and -2.7 ‰, respectively. The  $\delta D$  of groundwater in Well 3 was -11  
307 ‰ and the  $\delta^{18} O$  was -3.3 ‰. The  $\delta D$  of water in Dr. Creek ranged between -14 and -13 ‰ and  
308 averaged -14 ‰ and the  $\delta^{18} O$  ranged between -3.4 and -3.2 ‰ and averaged  $-3.3 \pm 0.1$  ‰.

309

310 *4.2.2. Salinity, calcium and magnesium*

311 The salinity in Well 1 ranged from 1.2 to 1.3 psu and averaged  $1.2 \pm 0.04$  psu (Table 1). Well  
312 2 had salinity of 0.2 and Well 3 had a salinity of 1.2 psu. The salinity in Dr. Creek ranged from  
313 0.3 to 0.5 psu, with a mean of  $0.4 \pm 0.04$  psu (Table 1).

314 The EC in Well 1 ranged from 2320 to 2499  $\mu S/cm$  and averaged  $1.2 \pm 0.04$   $\mu S/cm$  (Table 1).  
315 Well 2 had an EC of 399 and Well 3 had a salinity of 825  $\mu S/cm$ . The salinity in Dr. Creek  
316 ranged from 679 to 924  $\mu S/cm$ , with a mean of  $822 \pm 77$   $\mu S/cm$  (Table 1).

317 The  $Ca^{2+}$  concentrations in Well 1 ranged from 3.2 to 3.3 mg/L and averaged  $3.2 \pm 0.06$   
318 mg/L. The  $Ca^{2+}$  concentrations were 7.2 mg/L in Well 2 and 9.0 mg/L in Well 3. The  $Mg^{2+}$   
319 concentrations in Well 1 varied between 2.0 and 2.3 mg/L and averaged  $2.1 \pm 0.1$  mg/L. The  
320  $Mg^{2+}$  concentrations in Well 2 was 6.5 mg/L and in Well 3, the  $Mg^{2+}$  concentration was at 7.9  
321 mg/L. The  $Mg^{2+} /Ca^{2+}$  ratios varied between 0.6 and 0.9 in groundwater from Well 1, Well 2

322 and Well 3. The  $\text{Ca}^{2+}$  concentrations in Dr. Creek varied between 1.4 and 2.4 mg/L and  
323 averaged  $1.9 \pm 0.3$  mg/L. The  $\text{Mg}^{2+}$  concentrations in Dr. Creek ranged of 12.0 to 17.1 mg/L and  
324 averaged  $14.4 \pm 1.7$  mg/L. The  $\text{Mg}^{2+} / \text{Ca}^{2+}$  ratios in Dr. Creek varied from 6.2 to 8.3.

325

326 **5. Discussion**

327 5.1. Assessing tide-induced groundwater salinization

328 The EC in the coastal groundwater sampled in the Youpwe neighborhood in Douala,  
329 Cameroon ranged from 399 to 2499  $\mu\text{S}/\text{cm}$  (Table 1). The EC exceeded the WHO drinking water  
330 limit of 750  $\mu\text{S}/\text{cm}$  for drinking water (WHO 2004). The salinized groundwater observation is  
331 consistent with the results of previous studies that show highly salinized groundwater in the  
332 Douala coastal aquifer (Takem et al., 2010; Takem et al., 2015; Fantong et al., 2016; Ketchemen-  
333 Tandia et al., 2017; Wirmvem et al., 2017a). We use our time series groundwater and estuarine  
334 water salinity and temperature and the stable water isotopes, salinity and ionic ratios to assess if  
335 the origin of salinity that impairs the groundwater quality in the coastal aquifer in Douala  
336 Cameroon is tidally induced.

337

338 *5.1.1. Evaluation of tidal-induced groundwater salinization from temporal salinity and  
339 temperature variations*

340 Tidal intrusion of estuarine water into coastal aquifers that causes salinization occurs during  
341 high tides when estuarine water (1) has a higher head which induces flow of saline water into the  
342 groundwater aquifer where groundwater has a lower head and/or (2) overtops the topography and  
343 cause flooding and seepage of saline estuarine water into the groundwater aquifer (Mao et al.,  
344 2001; Mao et al., 2006; Lenkopane et al., 2009; Tularam and Singh, 2009; Shalem et al., 2019).

345 Tidal intrusion of saline water into coastal aquifers will induce concomitant or rhythmic cyclicity  
346 in groundwater levels and chemistry (Wang and Tsay, 2001; Lenkopane et al., 2009; Mitra et al.,  
347 2011). To track groundwater salinization due to tidal forcing, we compare the time series  
348 variations in water level (tides), salinity and temperature in estuarine water from Dr. Creek and  
349 the adjacent groundwater aquifer in Youpwe (Fig. 2). Similar to water in Dr. Creek, groundwater  
350 level increases and decreases coincide with the semidiurnal mixed tidal forcing in the Wouri  
351 Estuary (Fig. 2a vs. 2b). The variations in salinity in Dr. Creek (Fig. 2d) corresponds to tidal  
352 cycles (Fig. 2b), while the temporal salinity in groundwater (Fig. 2c) does not correspond to tidal  
353 cycles (Fig. 2a). This disparity between the behavior of tides and the temporal salinity in  
354 groundwater allows us to argue that shallow coastal groundwater at a distance of 120 m from the  
355 estuary is not affected by tide-induced salinization. Because tides are rhythmic, over time, the  
356 effect of tidal salinization should show a rhythmic behavior in the nearshore groundwater  
357 (Shalem et al., 2019).

358 It is clear that the temperature in Dr. Creek (Fig. 2f) only slightly mimics the sinusoidal  
359 patterns of tides (Fig 2b), with slight temperature decreases at high tide. On the other hand,  
360 groundwater temperature (Fig. 2e) mimics neither the behavior of the air temperature (Fig. 2g)  
361 nor Dr. Creek water temperature (Fig. 2f). The nearly constant temperature (temporal difference  
362 of 0.1 ° C; Table S1) in groundwater indicates that groundwater temperature is not affected by  
363 mixing with warmer surface water (temperature range 1.4 ° C; Table S1) from Dr. Creek. We  
364 posit that groundwater level fluctuations (Fig. 2a) which coincided with tidal cycles in Dr. Creek  
365 (Fig. 2b) is due to the effects of tidal energy, and not from the intrusion or infiltration of  
366 estuarine water into the groundwater (e.g., Wang and Tsay, 2001).

367

368     *5.1.2. Cause of groundwater salinization from isotopic and hydrochemical tracers*

369     The  $\delta^{18}\text{O}$  and  $\delta\text{D}$  and salinity are conservative, and are therefore good indicators of  
370     salinization by evapoconcentration and tracers of mixing between fresh groundwater and saline  
371     estuarine water (Kim et al., 2003; Bouchaou et al., 2008; Mongelli et al., 2013; Cary et al., 2015;  
372     Bahir et al., 2018; Carreira et al., 2018; Amiri et al., 2016). The  $\delta^{18}\text{O}$  and  $\delta\text{D}$  of water from Dr.  
373     Creek, groundwater in the Youpwe neighborhood and the Wouri River water (Wirmvem et al.,  
374     2017a) co-vary (Fig. 3a), cluster along the LMWL of Douala (Wirmvem et al., 2017b), and plot  
375     above the GMWL (Craig, 1961). The clustering of groundwater samples along the LMWL  
376     indicates meteoric origin of the groundwater (Ketchemen-Tandia et al., 2007; Wirmvem et al.,  
377     2017b).

378     Evidence for evapoconcentration in increasing solute concentrations, and therefore  
379     responsible for groundwater salinization by evapoconcentration can be assessed from the  
380     relationship between salinity and d-excess (Fig. 3b). Lower d-excess values indicate greater  
381     extent of evaporation (e.g., Dansgaard, 1964) which can be linked to salinization (e.g., Fröhlich  
382     et al., 2002; Huang and Pang, 2012; Krishan et al., 2020). The d-excess in groundwater, estuarine  
383     water in Dr. Creek and the Wouri River are between 11 and 15 and are in the range of 10 to 17  
384     observed in Douala precipitation (Wirmvem et al., 2017b) indicating a meteoric origin. The wide  
385     range in d-excess with a relatively limited variation in salinity is an indication of minimal effect  
386     of evaporation, consistent with unevaporated rain recharge of groundwater, short residence time  
387     of water in the creek and river and/or low evaporation rates from high humidity (Fantong et al.,  
388     2016).

389     We can use the relationship between salinity and  $\delta^{18}\text{O}$  (Fig. 4a) to assess saline estuarine  
390     water intrusion and mixing with groundwater (e.g., Gonfiantini and Araguás, 1988; Bahir et al.,

391 2018). In Figure 4a, we show a model line of freshwater (salinity = 0;  $\delta^{18}\text{O} = -2.9\text{ ‰}$ ) and  
392 seawater (salinity = 35;  $\delta^{18}\text{O} = 0\text{ ‰}$ ) end member mixing. We also show a line that depicts  
393 dissolution and leaching in freshwater with a  $\delta^{18}\text{O} = -2.9\text{ ‰}$ . The arrow showing increasing  
394 salinity indicates that the dissolution and leaching processes do not modify the  $\delta^{18}\text{O}$   
395 composition of water (Gonfiantini and Araguás, 1988). Both model lines have a  $\delta^{18}\text{O}$  end  
396 member value of -2.9 ‰, which represents the average  $\delta^{18}\text{O}$  composition of groundwater in  
397 Douala. On the salinity vs.  $\delta^{18}\text{O}$  plot, the data points from Dr. Creek, the Wouri River  
398 (Wirmvem et al., 2017a), coastal groundwater from Youpwe and the rest of the Douala coastal  
399 aquifer (Fantong et al., 2016) do not fall along the freshwater seawater mixing line (Fig. 4a),  
400 indicating no seawater intrusion. The groundwater samples that were analyzed from Well 1 were  
401 collected between low and high tide regimes (Fig. 2a), and yet, the data forms a cluster in the  
402 salinity vs.  $\delta^{18}\text{O}$  plot. This similarity of groundwater  $\delta^{18}\text{O}$  and salinity despite variations in  
403 collection times relative to tides indicates no systematic increases or decreases from tide-induced  
404 intrusion of estuarine water into groundwater. Similarly, estuarine water, Wouri River and  
405 groundwater are not affected by dissolution and/or leaching as the samples do not plot in the  
406 direction of the model line indicating dissolution and leaching (Fig. 4a).

407 The lack of seawater intrusion into the coastal aquifer is further supported by the  $\text{Mg}^{2+}/\text{Ca}^{2+}$   
408 vs. the electrical conductivity relationship (Fig. 4b). The  $\text{Mg}^{2+}/\text{Ca}^{2+}$  ratios should increase in  
409 groundwater with increased proportion of seawater intrusion where higher ratios ( $>1$ ) depict  
410 seawater intrusion, and lower ratios ( $<1$ ) indicate no seawater intrusion (Pulido-Leboeuf et al.,  
411 2003; Salem and Osman, 2017). The  $\text{Mg}^{2+}/\text{Ca}^{2+}$  of estuarine water from Dr. Creek range from  
412 6-8 and are much higher compared to groundwater (Fig. 4b). Groundwater from the coastal  
413 aquifer in Youpwe, as well as from the rest of the Douala coastal aquifer (Takem et al., 2010,

414 2015; Fantong et al., 2016) show low  $Mg^{2+}/Ca^{2+}$  ratios of  $<1$ , indicating no tide-induced  
415 salinization of groundwater (Fig. 4b).

416 The finding of no tide-induced groundwater salinization is inconsistent with the previous  
417 suggestion of possible seawater source for the high chloride concentrations observed in about  
418 30% of the shallow groundwater in the Douala aquifer located 0.44-3 km from the shoreline by  
419 Fantong et al. (2016). Fantong et al. (2016) argued that during high tides, seawater that flows  
420 through the Dibamba River and Wouri River cause bank overflow and flooding. The saline water  
421 from bank overflow and flooding recharges the unconfined shallow aquifer causing the high  
422 chloride concentrations observed. Although estuarine water overflow and flooding is able to  
423 salinize groundwater in close proximity to the rivers, Takem (2012) established from  $Na^+/Cl^-$   
424 ratios in groundwater in the Douala aquifer that less than 20% of samples had  $Na/Cl$  ratio lower  
425 than that of seawater, and argued against seawater intrusion as the primary source of the  
426 chloride. The widely distributed high chloride concentrations in groundwater of the Douala  
427 coastal aquifer was then attributed to sea spray aerosol and atmospheric sea salt deposition, as an  
428 alternative explanation to seawater intrusion (Takem et al., 2015). The salts deposited on the  
429 surface from the sea spray and atmospheric deposition are flushed by rain recharge into  
430 groundwater (Takem et al., 2015).

431 During our study, we observed tidal flooding at the surface adjacent to the groundwater  
432 sampling location, which can potentially induce saline water flow and/or recharge into the  
433 shallow groundwater. Moreover, the pumping of Well 1 at  $4.7\text{ m}^3/\text{s}$  should have further  
434 promoted lower groundwater head (which was decreased by 1.5 m) and facilitated salinization  
435 from inflow of estuarine water with a higher head. However, the  $Mg^{2+}/Ca^{2+}$  ratios of  $<1$  in  
436 groundwater is consistent with results from Takem (2012) that indicated that the high chloride

437 concentrations in the Douala coastal aquifer are not from modern seawater from the Gulf of  
438 Guinea. Our results do not support the Takem et al. (2015) idea of a sea spray origin for the high  
439 chloride concentrations in groundwater either. We make this argument because the ratio of the  
440 ions (e.g.,  $Mg^{2+}/Ca^{2+}$ ) in sea spray or sea salt deposition will be the same as in the seawater. If  
441 the sea spray or salt deposition was responsible for the high chloride concentrations in  
442 groundwater, we should observe  $Mg^{2+}/Ca^{2+}$  ratios  $\gg 1$ , which is not the case for groundwater  
443 in Youpwe neighborhood and the rest of the Douala coastal aquifer (Fig. 4b). Wirmvem et al.  
444 (2017a) posit that the main source of chloride in groundwater in the Douala coastal aquifer is  
445 from seepage from the numerous pit latrines in the city. Although our current study is unable to  
446 test this idea of anthropogenic pollution, we do observe higher salinity values ( $\sim 1$  psu) in  
447 groundwater (Well 1 and Well 3) (Fig. 3b) which can be attributed to either aquifer source of  
448 contamination or anthropogenic pollution.

449

## 450 **6. Conclusions**

451 We assessed tide-induced salinization in coastal groundwater in the Youpwe neighborhood in  
452 Douala which is adjacent to the Wouri Estuary in Cameroon. We employed a combination of  
453 time series investigations of water level (tides), salinity and temperature, and assessments of  
454 major cations and  $\delta^{18}O$  and  $\delta D$  in estuarine water and in groundwater. During our experiment,  
455 we pumped groundwater to decrease its head and to induce flow from estuarine water with  
456 higher head. Groundwater table showed tidal induced fluctuations similar to flood and tide ebb  
457 in the estuary. The salinity,  $\delta^{18}O$  and  $\delta D$  and  $Mg^{2+}/Ca^{2+}$  used as tracers showed salinity in  
458 groundwater did not originate from seawater and that there was no evidence of mixing between  
459 saline water in the estuary and groundwater. Thus, our results show that shallow groundwater

460 120-250 m from the estuary coast and groundwater in the broader Douala coastal aquifer in  
461 general is not affected by tidal-induced salinization. Our findings indicate that in estuarine  
462 settings where tidal salinization is not a major process controlling groundwater quality, other  
463 processes such as anthropogenic pollution and/or contamination from the aquifer formation  
464 (connate water in the aquifer units) that may affect groundwater quality should not be ignored.

465

#### 466 **Acknowledgments**

467 We thank the government of Cameroon (Ministry of Water Resources and Energy) for granting  
468 us research permits. We thank the manager and staff of the Aquarius Marina 2000 Hotel and two  
469 anonymous individuals for allowing access to their wells to conduct this study. We thank the  
470 students participating in the 2019 US National Science Foundation International Research  
471 Experience for Students field season for their help in data acquisition. We thank two anonymous  
472 reviewers whose comments helped improve this manuscript.

473

#### 474 **CRedit authorship contribution statement**

475 **Goabaone J. Ramatlape**ng: Writing- original draft, Data Analysis, Methodology, Visualization.  
476 **Eliot A. Atekwana**: Writing-reviewing and editing, Supervision, Funding Acquisition,  
477 Conceptualization, Methodology. **Hendratta N Ali**: Writing-reviewing and editing, Funding  
478 Acquisition. **Isaac K. Njilah**: Writing-reviewing and editing. **Gustave R. N. Ndondo**: Writing-  
479 reviewing and editing.

480

#### 481 **Declaration of competing interest**

482 The authors declare that they have no known competing financial interests or personal  
483 relationships that could have appeared to influence the work reported in this paper.

484

485 **Disclosure statement**

486 No potential conflict of interest was reported by the authors

487

488 **Funding**

489 This work was supported by the National Science Foundation under Grant OISE-1827065.

490 **REFERENCES**

491 Alcalá, F. J., & Custodio, E. (2008). Using the Cl/Br ratio as a tracer to identify the origin of  
492 salinity in aquifers in Spain and Portugal. *Journal of Hydrology*, 359(1-2), 189-207.

493 Amiri, V., Nakhaei, M., Lak, R., & Kholghi, M. (2016). Geophysical, isotopic, and  
494 hydrogeochemical tools to identify potential impacts on coastal groundwater resources from  
495 Urmia hypersaline Lake, NW Iran. *Environmental Science and Pollution Research*, 23(16),  
496 16738-16760.

497 Amiri, V., Bhattacharya, P., & Nakhaei, M., (2021). The hydrogeochemical evaluation of  
498 groundwater resources and their suitability for agricultural and industrial uses in an arid area  
499 of Iran. *Groundwater for Sustainable Development*, 12, p.100527.

500 APHA (1985). Standard methods for the examination of water and wastewater, 16th edn.  
501 American Public Health Association, Washington DC

502 Aquilina, L., Ladouce, B., Dörfliger, N., Seidel, J. L., Bakalowicz, M., Dupuy, C., & Le Strat,  
503 P. (2002). Origin, evolution and residence time of saline thermal fluids (Balaruc springs,

504 southern France): implications for fluid transfer across the continental shelf. *Chemical*  
505 *Geology*, 192(1-2), 1-21.

506 Bahir, M., Ouazar, D., & Ouhamdouch, S. (2018). Characterization of mechanisms and  
507 processes controlling groundwater salinization in coastal semi-arid area using  
508 hydrochemical and isotopic investigations (Essaouira basin, Morocco). *Environmental*  
509 *Science and Pollution Research*, 25(25), 24992-25004.

510 Bahir, M., & Ouhamdouch, S. (2020). Groundwater quality in semi-arid environments  
511 (Essaouira Basin, Morocco). *Carbonates and Evaporites*, 35(2), 1-16.

512 Bennett, A. S. (1976). Conversion of in situ measurements of conductivity to salinity. In *Deep*  
513 *Sea Research and Oceanographic Abstracts* (Vol. 23, No. 2, pp. 157-165). Elsevier.

514 Bouchaou, L., Michelot, J. L., Vengosh, A., Hsissou, Y., Qurtobi, M., Gaye, C. B., & Zuppi, G.  
515 M. (2008). Application of multiple isotopic and geochemical tracers for investigation of  
516 recharge, salinization, and residence time of water in the Souss–Massa aquifer, southwest of  
517 Morocco. *Journal of Hydrology*, 352(3-4), 267-287.

518 Brand W. A. (2011). New reporting guidelines for stable isotopes – an announcement to isotope  
519 users. *Isotopes in Environmental and Health Studies*, 47(4), 535-536, DOI:  
520 10.1080/10256016.2011.645702.

521 Carreira, P. M., Bahir, M., Ouhamdouch, S., Fernandes, P. G., & Nunes, D. (2018). Tracing  
522 salinization processes in coastal aquifers using an isotopic and geochemical approach:  
523 comparative studies in western Morocco and southwest Portugal. *Hydrogeology*  
524 *Journal*, 26(8), 2595-2615.

525 Cary, L., Petelet-Giraud, E., Bertrand, G., Kloppmann, W., Aquilina, L., Martins, V., & Franzen,  
526 M. (2015). Origins and processes of groundwater salinization in the urban coastal aquifers

527 of Recife (Pernambuco, Brazil): a multi-isotope approach. *Science of the Total*  
528 *Environment*, 530, 411-429.

529 Craig, H. (1961). Isotopic variations in meteoric waters. *Science*, 133(3465), 1702-1703.

530 Currell, M. J., Dahlhaus, P., & Ii, H. (2015). Stable isotopes as indicators of water and salinity  
531 sources in a southeast Australian coastal wetland: identifying relict marine water, and  
532 implications for future change. *Hydrogeology Journal*, 23(2), 235-248.

533 Dansgaard, W., 1964. Stable isotopes in precipitation. *Tellus*, 16(4), pp.436-468.

534 Demirel, Z. (2004). The history and evaluation of saltwater intrusion into a coastal aquifer in  
535 Mersin, Turkey. *Journal of Environmental Management*, 70(3), 275-282.

536 Dieng, N. M., Orban, P., Otten, J., Stumpp, C., Faye, S., & Dassargues, A. (2017). Temporal  
537 changes in groundwater quality of the Saloum coastal aquifer. *Journal of Hydrology: Regional Studies*, 9, 163-182.

538

539 Djeuda-Tchapnga, H. B., Tanawa, E., & Ngnikam, E. (2001). L'eau au Cameroun. *Presses*  
540 *Universitaires*, pp115-129.

541 Dumort, J. C. (1968). Notice explicative sur la feuille Douala-Ouest. *Direction Mines et de la*  
542 *Geologie du Cameroun, Yaounde.*

543 Fantong, W. Y., Kamtchueng, B. T., Ketchemen-Tandia, B., Kuitcha, D., Ndjama, J., Fouepe, A.  
544 T & Ako, A. A. (2016). Variation of hydrogeochemical characteristics of water in surface  
545 flows, shallow wells, and boreholes in the coastal city of Douala (Cameroon). *Hydrological*  
546 *Sciences Journal*, 61(16), 2916-2929. Fröhlich, K., Gibson, J.J. & Aggarwal, P.K., 2002.  
547 Deuterium excess in precipitation and its climatological significance (No. IAEA-CSP--  
548 13/P). Fossi Fotsi, Y., Pouvreau, N., Brenon, I., Onguene, R., & Etame, J. (2019). Temporal

549 (1948–2012) and Dynamic Evolution of the Wouri Estuary Coastline within the Gulf of  
550 Guinea. *Journal of Marine Science and Engineering*, 7(10), 343.

551 Giménez- Forcada, E. (2010). *Dynamic of sea water interface using hydrochemical facies*  
552 *evolution diagram. Groundwater*, 48(2), 212-216.

553 Gonfiantini, R., & Araguás, L. (1988). Los isótopos ambientales en el estudio de la intrusión  
554 marina. In *Tecnología de la intrusión en acuíferos costeros* (pp. 135-190).

555 Harkness, J. S., Darrah, T. H., Warner, N. R., Whyte, C. J., Moore, M. T., Millot, R., &  
556 Vengosh, A. (2017). The geochemistry of naturally occurring methane and saline  
557 groundwater in an area of unconventional shale gas development. *Geochimica et*  
558 *Cosmochimica Acta*, 208, 302-334.

559 Hem, J. D. (1985). *Study and interpretation of the chemical characteristics of natural*  
560 *water* (Vol. 2254). Department of the Interior, US Geological Survey.

561 Huang, T. & Pang, Z., 2012. The role of deuterium excess in determining the water salinisation  
562 mechanism: A case study of the arid Tarim River Basin, NW China. *Applied Geochemistry*,  
563 27(12), pp.2382-2388.

564 Isawi, H., El-Sayed, M. H., Eissa, M., Shouakar-Stash, O., Shawky, H., & Mottaleb, M. S. A.  
565 (2016). Integrated geochemistry, isotopes, and geostatistical techniques to investigate  
566 groundwater sources and salinization origin in the Sharm EL-Sheikh Area, South Sinai,  
567 Egypt. *Water, Air, & Soil Pollution*, 227(5), 151.

568 Jones, B. F., Vengosh, A., Rosenthal, E., & Yechieli, Y. (1999). Geochemical investigations.  
569 In *Seawater intrusion in coastal aquifers—concepts, methods and practices* (pp. 51-71).  
570 Springer, Dordrecht.

571 Jørgensen, N. O., Andersen, M. S., & Engesgaard, P. (2008). Investigation of a dynamic  
572 seawater intrusion event using strontium isotopes ( $87\text{Sr}/86\text{Sr}$ ). *Journal of*  
573 *Hydrology*, 348(3-4), 257-269.

574 Kanagaraj, G., Elango, L., Sridhar, S. G. D., & Gowrisankar, G. (2018). Hydrogeochemical  
575 processes and influence of seawater intrusion in coastal aquifers south of Chennai, Tamil  
576 Nadu, India. *Environmental Science and Pollution Research*, 25(9), 8989-9011.

577 Ketchemen-Tandia, B., Boum-Nkot, S. N., Ebondji, S. R., Nlend, B. Y., Emvoutou, H., &  
578 Nzegue, O. (2017). Factors Influencing the Shallow Groundwater Quality in Four Districts  
579 with Different Characteristics in Urban Area (Douala, Cameroon). *Journal of Geoscience*  
580 and *Environment Protection*, 5(08), 99.

581 Ketchemen-Tandia, B., Ntamak-Nida, M. J., Boum-Nkot, S., Wonkam, C., Emvoutou, H., &  
582 Ebonji Seth, C. R. (2007, May). First results of the isotope study ( $18\text{O}$ ,  $2\text{H}$ ,  $3\text{H}$ ) of the  
583 Douala Quaternary aquifer (Cameroon). In *IAEA Advances in isotope hydrology and its role*  
584 *in sustainable water resources management (HIS-2007). Proceedings of a symposium* (Vol.  
585 2, pp. 37-48).

586 Kim, Y., Lee, K. S., Koh, D. C., Lee, D. H., Lee, S. G., Park, W. B., & Woo, N. C. (2003).  
587 Hydrogeochemical and isotopic evidence of groundwater salinization in a coastal aquifer: a  
588 case study in Jeju volcanic island, Korea. *Journal of Hydrology*, 270(3-4), 282-294.

589 Krishan, G., Prasad, G., Kumar, C.P., Patidar, N., Yadav, B.K., Kansal, M.L., Singh, S., Sharma,  
590 L.M., Bradley, A. & Verma, S.K., 2020. Identifying the seasonal variability in source of  
591 groundwater salinization using deuterium excess-a case study from Mewat, Haryana, India.  
592 *Journal of Hydrology: Regional Studies*, 31, p.100724.

593 Lee, J. Y., & Song, S. H. (2007). Evaluation of groundwater quality in coastal areas: implications  
594 for sustainable agriculture. *Environmental Geology*, 52(7), 1231-1242.

595 Lenkopane, M., Werner, A. D., Lockington, D. A., & Li, L. (2009). Influence of variable salinity  
596 conditions in a tidal creek on riparian groundwater flow and salinity dynamics. *Journal of*  
597 *Hydrology*, 375(3-4), 536-545.

598 Mafany, G. T. (1999). Impact of the geology and seawater intrusion on groundwater quality in  
599 Douala. *Unpublished MSc Thesis, Department of Geology and Environmental Science,*  
600 *University of Buea, Cameroon.*

601 Mao, X., Enot, P., Barry, D. A., Li, L., Binley, A., & Jeng, D. S. (2006). Tidal influence on  
602 behaviour of a coastal aquifer adjacent to a low-relief estuary. *Journal of Hydrology*, 327(1-  
603 2), 110-127.

604 Mao, Z., Shen, H., Liu, T. J., & Eisma, D. (2001). Types of saltwater intrusion of the Changjiang  
605 Estuary. *Science in China Series B: Chemistry*, 44(1), 150-157.

606 Melloul, A. J., & Goldenberg, L. C. (1997). Monitoring of seawater intrusion in coastal aquifers:  
607 basics and local concerns. *Journal of Environmental Management*, 51(1), 73-86.

608 Mirzavand, M., Ghasemieh, H., Sadatinejad, S. J., & Bagheri, R. (2020). An overview on source,  
609 mechanism and investigation approaches in groundwater salinization studies. *International*  
610 *Journal of Environmental Science and Technology*, 1-14.

611 Mirzavand, M., Ghasemieh, H., Sadatinejad, S. J., Bagheri, R., & Clark, I. D. (2018). Saltwater  
612 intrusion vulnerability assessment using AHP-GALDIT model in Kashan plain aquifer as  
613 critical aquifer in a semi-arid region. *Desert*, 23(2), 255-264.

614 Mitra, A., Mondal, K., & Banerjee, K. (2011). Spatial and Tidal Variations of Physico-Chemical  
615 Parameters in the Lower Gangetic Delta Region, West Bengal, India. *Journal of Spatial*  
616 *Hydrology*, 11(1).

617 Mongelli, G., Monni, S., Oggiano, G., Paternoster, M., & Sinisi, R. (2013). Tracing groundwater  
618 salinization processes in coastal aquifers: a hydrogeochemical and isotopic approach in Na-  
619 Cl brackish waters of north-western Sardinia, Italy. *Hydrology & Earth System Sciences*  
620 *Discussions*, 10(1).

621 Ndongo, B., Mbouendeu, S. L., Tirmou, A. A., Njila, R. N., & Dalle, J. D. M. (2015). Tendances  
622 pluviométriques et impact de la marée sur le drainage en zone d'estuaire: cas du Wouri au  
623 Cameroun. *Afrique Science: Revue Internationale des Sciences et Technologie*, 11(2), 173-  
624 182.

625 Ngon, G. F. N., Etame, J., Ntamak-Nida, M. J., Mbisse, C. O., Mbai, J. S., Bayiga, É. C., &  
626 Gerard, M. (2016). Geochemical and palaeoenvironmental characteristics of Missole I iron  
627 duricrusts of the Douala sub-basin (Western Cameroon). *Comptes Rendus*  
628 *Geoscience*, 348(2), 127-137.

629 Olivry, J. C. (1974). L'alimentation en eau de Douala, hydrologie du bief maritime de la  
630 Dibamba en période d'étiage: Note sur les étiages du Mungo.

631 Onguene, R., Pemha, E., Lyard, F., Du-Penhoat, Y., Nkoue, G., Duhaut, T., & Allain, D. (2014).  
632 Overview of Tide Characteristics in Cameroon Coastal Areas Using Recent  
633 Observations. *Open Journal of Marine Science*, 5(01), 81.

634 Ouhamdouch, S., Bahir, M., & Carreira, P. M. (2017). Geochemical and isotopic tools to  
635 deciphering the origin of mineralization of the coastal aquifer of Essaouira basin,  
636 Morocco. *Procedia Earth and Planetary Science*, 17, 73-76.

637 Ouhamdouch, S., Bahir, M., & Ouazar, D. (2021). Seawater intrusion into coastal aquifers from  
638 semi-arid environments, Case of the alluvial aquifer of Essaouira basin  
639 (Morocco). *Carbonates and Evaporites*, 36(1), 1-12.

640 Pulido-Laboeuf, P. (2004). Seawater intrusion and associated processes in a small coastal  
641 complex aquifer (Castell de Ferro, Spain). *Applied geochemistry*, 19(10), 1517-1527.

642 Pulido-Leboeuf, P., Pulido-Bosch, A., Calvache, M. L., Vallejos, Á., & Andreu, J. M. (2003).  
643 Strontium,  $\text{SO}_4^{2-}/\text{Cl}^-$  and  $\text{Mg}^{2+}/\text{Ca}^{2+}$  ratios as tracers for the evolution of seawater into  
644 coastal aquifers: the example of Castell de Ferro aquifer (SE Spain). *Comptes Rendus  
645 Geoscience*, 335(14), 1039-1048.

646 Regnoult, J. M. (1986). *Synthèse géologique du Cameroun* (p. 119). Ministère des mines et de  
647 l'energie.

648 Salem, Z. E. S., & Osman, O. M. (2017). Use of major ions to evaluate the hydrogeochemistry of  
649 groundwater influenced by reclamation and seawater intrusion, West Nile Delta,  
650 Egypt. *Environmental Science and Pollution Research*, 24(4), 3675-3704.

651 Shalem, Y., Yechiali, Y., Herut, B., & Weinstein, Y. (2019). Aquifer response to estuarine  
652 stream dynamics. *Water*, 11(8), 1678.

653 Simon, L. N., & Raffaelli, D. (2012). Assessing ecosystem effects of small scale cutting of  
654 Cameroon mangrove forests. *Journal of Ecology and the Natural Environment*, 4(5), 126-  
655 134.

656 Slater, C., Preston, T. and Weaver, L.T. (2001). Stable isotopes and the international system of  
657 units. *Rapid Communications in Mass Spectrometry*, 15(15), pp.1270-1273.

658 Takem, G. E. (2012). Hydrogeochemistry and pollution characteristics of the unconfined urban  
659 aquifer of the city of Douala-Cameroon: implications for shallow groundwater management  
660 and use (Doctoral dissertation, PhD thesis, University of Buea).

661 Takem, G. E., Chandrasekharam, D., Ayonghe, S. N., & Thambidurai, P. (2010). Pollution  
662 characteristics of alluvial groundwater from springs and bore wells in semi-urban informal  
663 settlements of Douala, Cameroon, Western Africa. *Environmental Earth Sciences*, 61(2),  
664 287-298.

665 Takem, G. E., Kuitcha, D., Ako, A. A., Mafany, G. T., Takounjou-Fouepe, A., Ndjama, J., &  
666 Ayonghe, S. N. (2015). Acidification of shallow groundwater in the unconfined sandy  
667 aquifer of the city of Douala, Cameroon, Western Africa: implications for groundwater  
668 quality and use. *Environmental Earth Sciences*, 74(9), 6831-6846.

669 Tamfu, S., Batupe, M., Pauken, R. J., & Boatwright, D. C. (1995). Geologic setting, stratigraphy  
670 and hydrocarbon habitat of the Douala Basin Cameroon. *National Hydrocarbon Journal of*  
671 *Cameroon*, 3(6).

672 Tularam, G. A., & Singh, R. (2009). Estuary, river and surrounding groundwater quality  
673 deterioration associated with tidal intrusion. *Journal of Applied Sciences in Environmental*  
674 *Sanitation*, 4(2), 141-150.

675 Wang, J., & Tsay, T. K. (2001). Tidal effects on groundwater motions. *Transport in Porous*  
676 *Media*, 43(1), 159-178.

677 Werner, A. D., Bakker, M., Post, V. E., Vandenbohede, A., Lu, C., Ataie-Ashtiani, B., & Barry,  
678 D. A. (2013). Seawater intrusion processes, investigation and management: recent advances  
679 and future challenges. *Advances in Water Resources*, 51, 3-26.

680 WHO (2011) Guidelines for drinking-water quality, 4<sup>th</sup> edition. Geneva, Switzerland

681 Wirmvem, M. J., Ohba, T., Nche, L. A., Kamtchueng, B. T., Kongnso, W. E., Mimba, M. E., &  
682 Ako, A. A. (2017a). Effect of diffuse recharge and wastewater on groundwater  
683 contamination in Douala, Cameroon. *Environmental Earth Sciences*, 76(9), 354.  
684 Wirmvem, M. J., Ohba, T., Kamtchueng, B. T., Taylor, E. T., Fantong, W. Y., & Ako, A. A.  
685 (2017b). Variation in stable isotope ratios of monthly rainfall in the Douala and Yaounde  
686 cities, Cameroon: local meteoric lines and relationship to regional precipitation  
687 cycle. *Applied Water Science*, 7(5), 2343-2356.

688

#### 689 **Table Captions**

690 **Table 1:** Station type, station location, stable isotopes of hydrogen ( $\delta D$ ) and oxygen ( $\delta^{18} O$ ),  
691 salinity, electrical conductivity (EC),  $Mg^{2+}$ ,  $Ca^{2+}$ , total iron, nitrate, phosphate and ammonia  
692 measured in shallow coastal groundwater (Well 1, 2, 3) in Youpwe, Douala and in Dr. Creek in  
693 the Wouri Estuary.

694

#### 695 **Figure Captions**

696 **Figure 1:** Figure 1: (a) Insert showing the map of the Wouri Estuary in Douala Cameroon,  
697 Africa and the sampling location (yellow square), (b) Google earth image showing the sampling  
698 locations along Dr. Creek in the Wouri Estuary near the Youpwe neighborhood in Douala. (c) a  
699 zoomed in insert showing groundwater sampling locations in Youpwe.

700

701 **Figure 2:** Temporal relative water level (a, b), salinity (c, d), and temperature (e, f) in  
702 groundwater (Well 1) in Youpwe and in Dr. Creek in the Wouri estuary and air temperature (g,  
703 h) in Youpwe.

704

705 **Figure 3:** Figure 3: Cross plot of (a)  $\delta^{18}\text{O}$  vs.  $\delta\text{D}$  and (b) salinity vs. d-excess for water samples  
706 from Dr. Creek and coastal groundwater (Well 1, 2, 3) from Youpwe and Wouri River water  
707 samples (Wirmvem et al., 2017a). Also shown on the plot are the Global Meteoric Water Line  
708 (GMWL; Craig, 1961) and Local Meteoric Water Line (LMWL) of Douala (Wirmvem et al.,  
709 2017b).

710

711 **Figure 4:** Cross plot of (a) Salinity vs.  $\delta^{18}\text{O}$  and (b)  $\text{Mg}^{2+}/\text{Ca}^{2+}$  ratios vs. Electrical  
712 conductivity (EC) for samples from Dr. Creek and groundwater (Well 1, 2, 3). Also shown are  
713 groundwater samples from the Fantong et al. (2016) study and river water samples from Wouri  
714 River (Wirmvem et al., 2017ba. The freshwater-seawater mixing line and change in salinity  
715 from the dissolution and leaching process are shown. Adapted from Gonfiantini and Araguás-  
716 Araguás (1988).

717

718

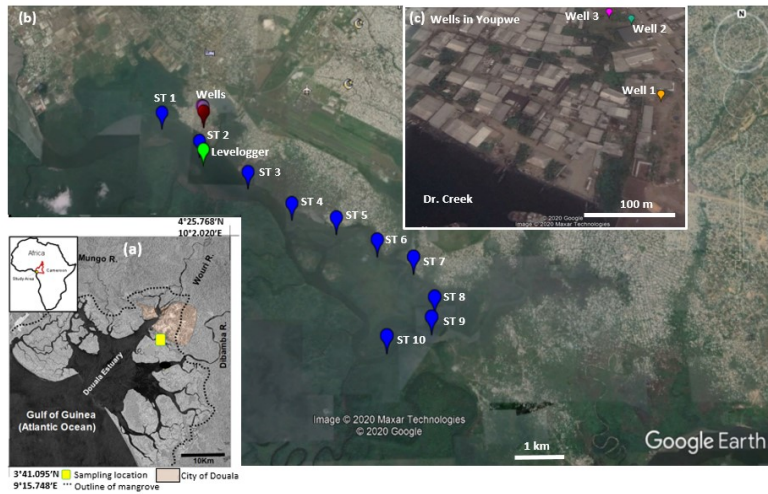


**Figure 1:** (a) Insert showing the map of the Wouri Estuary in Douala Cameroon, Africa and the sampling location (yellow square), (b) Google earth image showing the sampling locations along Dr. Creek in the Wouri Estuary near the Youpwe neighborhood in Douala. (c) a zoomed in insert showing groundwater sampling locations in Youpwe.

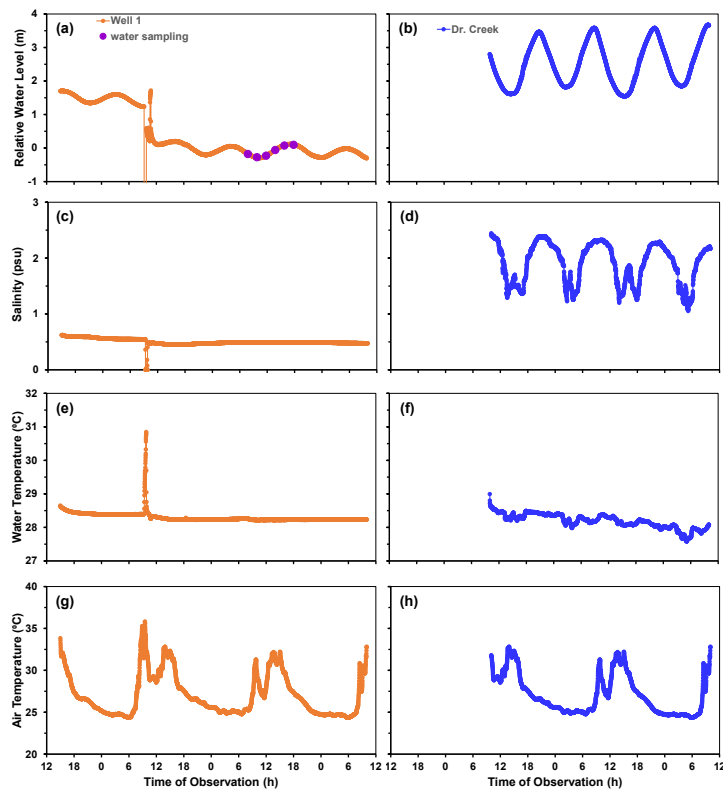


**Figure 2:** Temporal relative water level (a, b), salinity (c, d), and temperature (e, f) in groundwater (Well 1) in Youpwe and in Dr. Creek in the Wouri estuary and air temperature (g, h) in Youpwe.

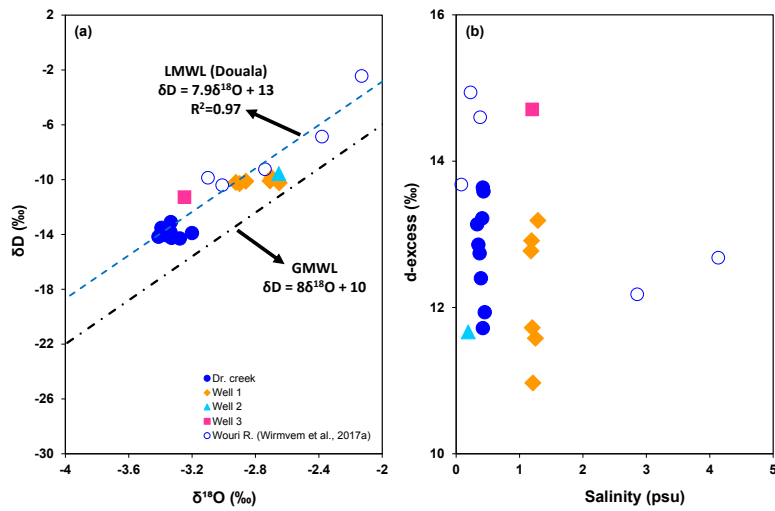


**Figure 3:** Cross plot of (a)  $\delta^{18}\text{O}$  vs.  $\delta D$  and (b) salinity vs. d-excess for water samples from Dr. Creek and coastal groundwater (Well 1, 2, 3) from Youpwe and Wouri River water samples (Wirmvem et al., 2017a). Also shown on the plot are the Global Meteoric Water Line (GMWL; Craig, 1961) and Local Meteoric Water Line (LMWL) of Douala (Wirmvem et al., 2017b).

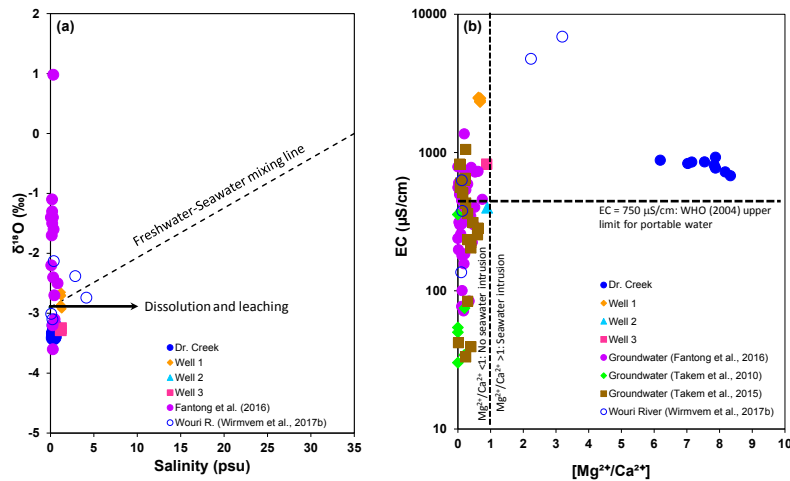


**Figure 4:** Cross plot of (a) Salinity vs.  $\delta^{18}\text{O}$  and (b)  $\text{Mg}^{2+}/\text{Ca}^{2+}$ ratios vs. Electrical conductivity (EC) for samples from Dr. Creek and groundwater (Well 1, 2, 3). Also shown are groundwater samples from the Fantong et al. (2016) study and river water samples from Wouri River (Wirmvem et al., 2017b). The freshwater-seawater mixing line and change in salinity from the dissolution and leaching process are shown. Adapted from Gonfiantini and Araguás-Araguás (1988).